Journal of The Electrochemical Society, **159** (1) C25-C28 (2012)
0013-4651/2012/159(1)/C25/4/$28.00 © The Electrochemical Society

Synthesis and Optical Properties of Iridescent Porous Anodic Alumina Thin Films

Qin Xu, Yu-Hua Yang, Li-Hu Liu, Jian-Jun Gu, Jing-Jin Liu, Zi-Yue Li, and Hui-Yuan Sun[z]

College of Physics Science & Information Engineering, Hebei Normal University, and Key Laboratory of Advanced Films of Hebei Province, Shijiazhuang 050016, China

Highly ordered porous anodic alumina thin films with tunable structural colors covering the entire visible region have been fabricated using chemical etching. The relationship of the structural color to the anodization time and etching time in a phosphoric acid solution, as well as the angle of incidence of illuminating light are discussed. Multicolor patterns were obtained by an organics-assisted process. A theoretical study of the changes in structural color due to various factors is consistent with the experimental results. These films show promise in many areas including decoration, display and anti-counterfeiting applications.
© 2011 The Electrochemical Society. [DOI: 10.1149/2.016201jes] All rights reserved.

Manuscript submitted July 21, 2011; revised manuscript received September 6, 2011. Published December 6, 2011.

Color production in nature is usually based on either structural color or pigmentation. Structural colors in insects and bird feathers have long attracted the attention of biologists due to their many useful characters including iridescence, high reflectivity and polarization. In recent years, a large amount of experimental work, especially on the microscopic and submicroscopic levels, has been undertaken to clarify the relationship between the brilliant colors and the microstructures involved.[1–4] These extensive studies have now progressed to the point where there are numerous applications in many industrial fields such as painting, automobiles, cosmetics, display technologies and textiles.

Recently, this research has revealed that even very simple natural structures can have surprising multiple functions,[5,6] and many researchers have attempted to replicate biological structures.[7–12] For instance, Lezec et al.[13] reported the fabrication of submicron, periodic dimple arrays on reflective silicon surfaces that may find a wide range of applications where low-reflectivity surfaces are required. Diggle et al.[14] have reported that a thin porous anodic alumina (PAA) thin film supported on an Al substrate produces, on reflection, a bright color in the visible light range due to the interference of the reflected light. Such a surface with unique reflectance properties could be useful for decoration and for anti-counterfeiting. Zhao et al.[15] constructed a PAA film embedded with carbon nanotubes (CNTs@PAA) on an Al substrate and found that infusion with water resulted in a significant color change. Such films might be used as water sensors. Finally, Wang et al.[16] reported that brilliant carbon-coated PAA thin films on an Al substrate were useful not only for weather-resistant decorative purposes, but also showed promise as effective broadband optical limiters for nanosecond laser pulses.

It is worth noting that all the above films were supported on an Al substrate, which limits the applications to some extent. Moreover, since Al has high reflectivity for visible light, the Al substrate will tend to lead to structural colors that are far from being saturated. In this connection, CNTs@PAA composite films display brilliant colors due to the fact that the embedded carbon efficiently screens the reflected light from the Al substrate. For many applications, however, the inclusion of carbon nanotubes is a complexity to be avoided, and it is desirable to discuss the structural colors of PAA thin films in the absence of the Al substrate. However, to date, there have been no reported attempts to produce highly saturated colors using films of this type. In the present paper, we report the fabrication of PAA thin films with brilliant structural colors by means of electrochemical oxidation of Al and etching in phosphoric acid. We also discuss the dependence of the optical properties on the parameters of the fabrication as well as the manner of viewing the films.

In this paper, high-purity aluminum foils (99.999%) were annealed at 400°C for 2 hours in an argon atmosphere, and then were electropolished in a 1:4 (volume) mixture of $HClO_4$ and C_2H_5OH for 5 minutes. After a first anodization, carried out at a constant voltage of 45 V in 0.3 M oxalic acid at 5°C for 6 hours, the alumina film was chemically removed by immersing it in a mixture of phosphoric acid (6 wt %) and chromic acid (4 wt %) at 40°C for 8 hours. Subsequently, a second anodization was conducted for a few minutes under the same conditions as in the first step. Part of the sample was then etched in a saturated $CuCl_2$ solution that removed the remaining aluminum substrate and left a thin alumina film.

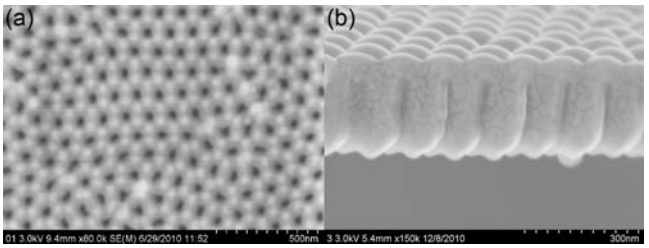

Figure 1. FE-SEM images of a PAA thin film anodized for 100 s, after removal of the Al substrate. (a) surface image and (b) cross section image.

The thin PAA films were characterized by field-emission scanning electron microscopy (FE-SEM, Hitachi S-570), and by an optical digital camera (Sony Dsc-T20) with a rough black cloth as the background. The morphology was observed using a scanning probe microscope (SPM, Veeco Nanoscope IV). UV-Vis diffuse reflectance spectra were recorded on a Hitachi UV-3010 spectrophotometer equipped with an integrating sphere. $BaSO_4$ was used as a reference.

Figure 1 shows FE-SEM images of the surface and cross section of a typical PAA thin film formed after a second anodization for 100 s. (See Experimental section). As shown in Figure 1a, a highly ordered nanopore array arranged in a close-packed hexagonal pattern can be clearly observed. The ordered pore arrays have identical pore diameters of about 25 nm, and an interpore spacing of approximately 125 nm. Figure 1b shows the cross section image from which the thicknesses of the PAA thin film can be directly measured to be about 200 nm. From these data, the pore growth rate of the PAA thin film during anodization can be estimated to be about 2 nm s^{-1}. The PAA films discussed in this article were prepared by adjusting the anodization time from 100 s to 160 s. The corresponding thicknesses of the films are shown in Table I, where t is anodized time, d the thickness of the film, and λ the reflected wavelength.

Table I. The character of PAA thin films.

t (s)	100	110	120	140	150	160
d (nm)	200	220	240	280	300	320
λ (nm)	419	461	502	586	628	670

[z] E-mail: huiyuansun@126.com

Downloaded on 2014-10-04 to IP 128.252.67.66 address. Redistribution subject to ECS terms of use (see ecsdl.org/site/terms_use) unless CC License in place (see abstract).

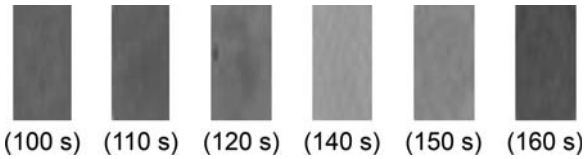

Figure 2. Colors of PAA thin films anodized from 100 s to 160 s.

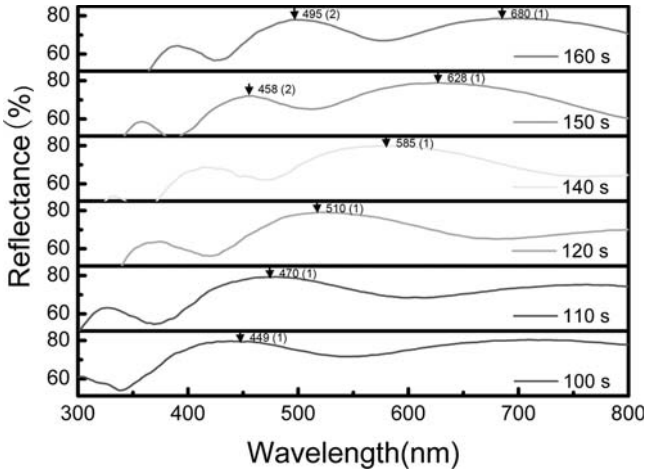

Figure 3. UV-Vis reflectance spectra of PAA thin films with different thicknesses and anodization times between 100 s to 160 s. The films show interference colors varying from purple to red.

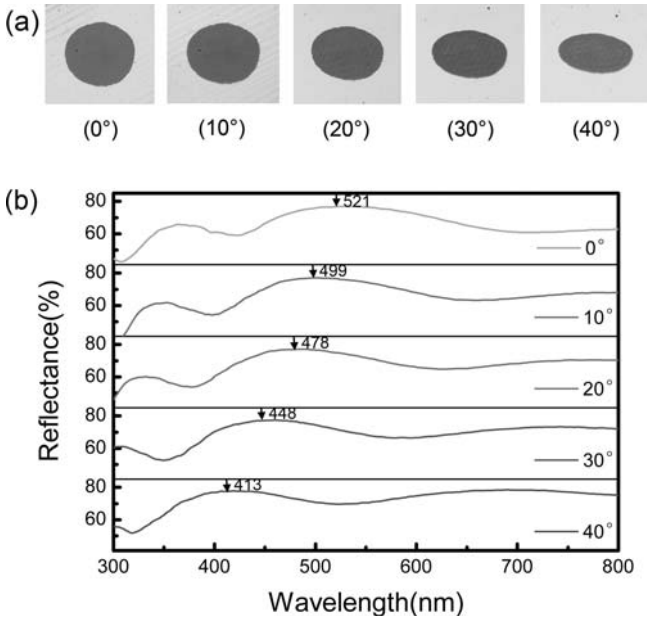

Figure 4. Photographs (a) and UV-Vis reflectance spectra (b) of the PAA film anodized for 125 s as observed using white light incident from different incident angles from 0° to 40°.

Figure 2 shows the colors of the films anodized for times ranging from 100 s to 160 s observed in natural light at nearly normal incidence, illustrating how the color gradually changes from violet to red as the anodization time is increased by 60 s. The structural color predominantly stems from the interference between light reflected from the top and bottom surfaces of the film. For free standing films, the phase of the light reflected from either the top or the lower surface of the film undergoes an addition phase change corresponding to a path difference of half a wavelength. Bragg's equation can then be written:

$$2nd\cos\theta = \left(m + \frac{1}{2}\right)\lambda \qquad [1]$$

where n is the refractive index of the film at a wavelength of λ, d the film thickness, θ the refraction angle, m the order of the interference, and λ the wavelength outside the film, respectively.

In our experiments, the effective refractive index was calculated to be about 1.57 according to Maxwell-Garnett theory.[17] The order of the interference can be estimated through film thickness and the corresponding maximum wavelength obtained by the experiment, here the order of the interference was one. So we can calculate the maximum reflected wavelength of the samples as shown in Table I, which is in good accordance with the observed color.

UV-Vis reflection spectra of PAA thin films with different thicknesses, all viewed at nearly normal incidence, are shown in Figure 3. It can be seen that the interference band with the maximum reflectance in the visible region shows a red shift with increasing anodization time. This indicates that wavelength of maximum reflection increases with increasing film thickness in accord with Bragg's equation. The calculated wavelengths listed in Table I correspond well with the experimental results indicated with vertical arrows at long-wave band. However, the calculated value is less than the experimental result at short-wave band due to the increasing of the refractive index.[16] For the film anodized for 160s, the reflection spectra appears the second peak besides the first peak at the visible range, and the wavelength of the second order of the interference still obeys the Bragg's equation.

The color not only changes with the anodization time, but also varies with the angle of incidence of the light used to view the film as shown in Figure 4a. It can be seen that the color of the PAA film changes from green to violet as the angle of incidence changes from 0° to 40°. Modulation of the reflectance spectra depending on the change of the incident angle is shown in Figure 4b. The maxima calculated using Bragg's equation are at 523 nm, 515 nm, 492 nm, 453 nm, and 401 nm, which is good agreement with the experimental results indicated with vertical arrows. This demonstrates that the above change is also consistent with Bragg's equation.

The pore growth rate of the PAA in the anodization is very fast, so it would be difficult to tune the color of the PAA thin film in a well-controlled manner. In order to obtain precise color tuning of the PAA thin films, it is necessary to reduce the thicknesses of the PAA films slowly. It has been reported that controllable precise color tuning of CNTs@PAA composite thin films can be achieved via phosphoric acid etching which not only reduces the film thickness, but also increases the diameter of the pores.[15] Likewise in our experiment PAA thin films exhibiting different colors can be obtained by etching with phosphoric acid at room temperature. The PAA films were floated on a 6 wt % phosphoric acid aqueous solution surface to make sure that only the back surface of PAA films came into contact with the solution. Photographs of PAA films anodized for 175 s but with different phosphoric acid etching times from 0 to 90 min are shown in Figure 5.

Figure 5. Photographs of the PAA thin film anodized for 175 s with different etching times from 0 to 90 min.

Downloaded on 2014-10-04 to IP 128.252.67.66 address. Redistribution subject to ECS terms of use (see ecsdl.org/site/terms_use) unless CC License in place (see abstract).

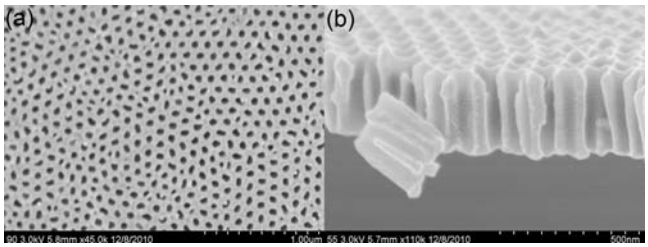

Figure 6. For the PAA thin film anodized for 175 s, (a) back side image with etching time of 90 min, and (b) cross section image with an etching time of 55 min.

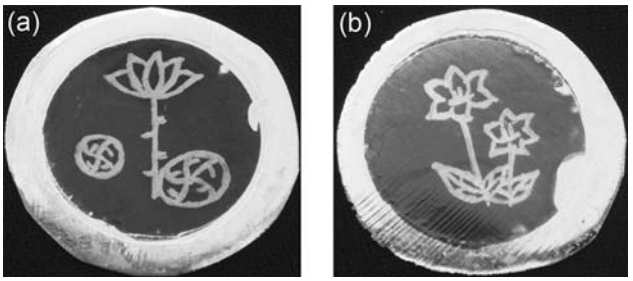

Figure 8. The patterns of the PAA thin films deposited with Co exhibit different colors.

It can be seen that the color changes from violet to blue over this time. It is important to note that initially, the color changes slowly, but subsequently changes more quickly. The initial slow color change for PAA films etched for shorter than 55 min can be attributed mainly to overall thinning of the film, while the faster color changes observed for etching times longer than 55 min is due to both thinning of the film and a decrease in the refractive index due an increase in the pore diameters.[15]

Further characterization of the above results was carried out by FE-SEM imagery. From Figure 6a, it may be observed that the PAA thin film which was etched for 90 min already presents an orderly array of holes that traverse the entire thickness of the film. The average pore diameter has increased to 60 nm after 90 min of phosphoric acid etching. Moreover, the porosity increase gives rise to a reduction in the refractive index.[18] The cross section of a PAA film anodized for 175 s after phosphoric acid etching for 55 min is shown in Figure 6b, illustrating the extent to which the pore diameter increases. The thickness of the film was approximately 295 nm, showing that the rate of etching in the phosphoric acid solution was about 1 nm min^{-1}, which is much lower than the rate of growth during anodization.

Such colored PAA thin films are useful for decoration and anti-counterfeiting technology, since a wide variety of patterns can be recorded on thin PAA films. A PAA thin film with a distinct pattern formed by anodizing different areas for different times is shown in the Figure 7a–7c, which clearly indicates that multicolor films can be fabricated via anodizing different areas of the aluminum foil. We obtained the pattern by covering part of the top surface of the PAA thin film with an ink pen before removal of the Al substrate, anodizing the uncovered part for a few seconds, and then repeating the above process, finally removing the ink with acetone. It can be seen that the pattern presents different colors across the visible spectrum. From the above discussion we know that different color corresponds to different thickness. The thickness of covered ink part is less than the uncovered part. Therefore, we characterized the interface of different color by a SPM, the results are shown in Figure 7d. It illustrates the change of the thickness across two areas of different color. These films have not been subjected to etching in phosphoric acid.

It is known that PAA templates can be used for depositing other metal material using electrochemical method. If the color still keeps after depositing metal, this will make up for the shortage of fragile. Therefore, we have fabricated Co@PAA nanocomposite films, and found that such colored films can be obtained by changing the deposited condition. At present, we have obtained some initial results in this area, as shown in Figure 8. In addition, such films have excellent magnetic properties combined with color. This suggests that the above nanocomposite materials may find application in multifunction anti-counterfeiting, in which the technology not only employs the optical properties, but also the functions of magnetic patterning. This technology would expand the range of potential applications of colored nancomposite films. Further experiments are under way to investigate nanocomposite magnetic materials.

In summary, the microstructure characteristics and optical properties of PAA thin films have been analyzed. The FE-SEM results confirmed that the structure has an ordered hexagonal pattern. Precise color tuning of the PAA thin films could be achieved by etching the films in phosphoric acid solution. It was found that the maxima of the reflected wavelengths in the UV-Vis reflectance spectra were consistent with the observed colors and with theoretical analysis.

Acknowledgments

This work is supported by the Natural Science Foundation of Hebei Province (Grant No. A2009000254), and the Ph.D. fund from Hebei Normal University (Grant No. L2006B10; No. L2009Y03). The authors wish to thank Dr. Norm Davison for helpful discussion.

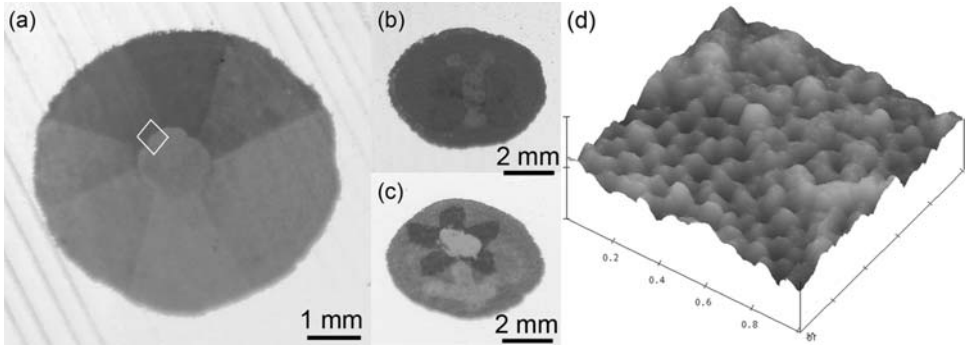

Figure 7. (a) Photograph of the PAA thin film with differently anodized areas, viewed in natural light. The anodization time was 10 s for each area after the purple area anodized for 100 s. Patterns of a butterfly (b) and a flower (c). (d) Three dimensional topographic image of the barrier layer side of the part of Figure 7a in the white rectangle area, exhibiting different thicknesses.

Downloaded on 2014-10-04 to IP 128.252.67.66 address. Redistribution subject to ECS terms of use (see ecsdl.org/site/terms_use) unless CC License in place (see abstract).

References

1. K. Mathias, M. S.–C. Pedro, R. J. S. Maik, H. Fumin, V. Pete, M. Sumeet, J. B. Jeremy, and S. Ullrich, *Nature Nanotechnology*, **5**, 511 (2010).
2. J. P. Vigneron, J.-F. Colomer, M. Rassart, A. L. Ingram, and V. Lousse, *Phys. Rev. E*, **73**, 021914 (2006).
3. O. Deparis, M. Rassart, C. Vandenbem, V. Welch, J. P. Vigneron, and S. Lucas, *New J. Phys.*, **10**, 013032 (2008).
4. X. Hu, Z. Y. Ling, T. L. Sun, and X. H. He, *J. Electrochem. Soc.*, **156**, D521 (2009).
5. P. Vukusic and J. R. Sambles, *Nature*, **424**, 852 (2003).
6. A. Argyros, S. Manos, M. C. J. Large, D. R. Mckenzie, G. C. Cox, and D. M. Dwarte, *Micron*, **33**, 483 (2002).
7. J. Y. Huang, X. D. Wang, and Z. L. Wang, *Nano Lett.*, **6**, 2325 (2006).
8. G. Y. Xie, G. M. Zhang, F. Lin, J. Zhang, Z. F. Liu, and S. C. Mu, *Nanotechnology*, **19**, 095605 (2008).
9. W. Zhang, D. Zhang, T. X. Fan, J. J. Gu, J. Ding, H. Wang, Q. X. Guo, and H. Ogawa, *Chem. Mater.*, **21**, 33 (2009).
10. X. Hu, Z. Y. Ling, X. H. He, and S. S. Chen, *J. Electrochem. Soc.*, **156**, C176 (2009).
11. A. R. Parker and H. E. Townley, *Nature Nanotechnology*, **2**, 347 (2007).
12. J. W. Galusha, M. R. Jorgensen, and M. H. Bartl, *Adv. Mater.*, **22**, 107 (2010).
13. H. J. Lezec, J. J. Mcmahon, O. Nalamasu, and P. M. Ajayan, *Nano Lett.*, **7**, 329 (2007).
14. J. W. Diggle, T. C. Downie, and C. W. Goulding, *Chen. Rev.*, **69**, 365 (1969).
15. X. L. Zhao, G. W. Meng, Q. L. Xu, F. M. Han, and Q. Huang, *Adv. Mater.*, **22**, 2637 (2010).
16. X. H. Wang, T. Akahane, H. Orikasa, T. Kyotani, and Y. Y. Fu, *Appl. Phys. Lett.*, **91**, 011908 (2007).
17. J. C. Maxwell Garnett, *Philos. Trans. R. Soc.*, **205**, 237 (1906).
18. S. Walheim, E. Schäffer, J. Mlynek, and U. Steiner, *Science*, **283**, 520 (1999).

Downloaded on 2014-10-04 to IP 128.252.67.66 address. Redistribution subject to ECS terms of use (see ecsdl.org/site/terms_use) unless CC License in place (see abstract).